

DISTORTIONS OF A LASER PULSE IN A RAMAN-SCATTERING MEDIUM

V.P. Sadovnikov, G.M. Strelkov, and M.F. Shalyaev

*Institute of Radio Engineering and Electronics,
Academy of Sciences of the USSR, Moscow*

Received August 11, 1989

The effect of stimulated Raman scattering (SRS) on the propagation of a laser pulse on horizontal atmospheric paths was studied numerically in the quasioptical approximation. It is shown that SRS strongly affects the redistribution of the energy in a powerful laser pulse between the incident radiation and the Stokes component. It was found that the profile of the Stokes beam changes along the path and spreads rapidly in space. The effect of SRS increases as the wavelength of the incident radiation decreases and it becomes only insignificantly weaker on high-altitude paths (up to 20 km).

Stimulated Raman scattering is of fundamental importance in the analysis of the transfer of high-power laser radiation through the atmosphere as well as in problems of laser sounding and monitoring of the atmosphere.^{1,2} Stimulated Raman scattering has been studied in many works on laser frequency conversion in cells and has virtually not been studied under the conditions of propagation of laser beams along extended paths in the real atmosphere. Stimulated Raman scattering of laser beams in the constituent gases of the atmosphere is studied theoretically in Refs. 3 and 4, but not for the actual atmospheric parameters. In addition, the attenuation of radiation along the direction of propagation is not taken into account. The attenuation of the components of the radiation must be taken into account on extended paths in the atmosphere since the attenuation coefficient for the Stokes component determines the threshold for SRS. In Ref. 1 it is shown that under the conditions of propagation of an intense laser beam along a path near the ground SRS strongly affects the redistribution of the energy in the pulse between the components of the radiation. In this paper the effect of SRS on the propagation of high-power laser beams on extended horizontal paths at altitudes H equal to 5 and 20 km above the earth's surface is studied.

The propagation of the radiation along the path is described by the equations for the complex amplitudes of the waves of the incident radiation (IR) ϵ_p and the Stokes component (SC) ϵ_s . The equations describe the diffraction of waves in space, their interaction in the process of SRS, and losses in the medium:

$$\frac{\partial \epsilon_p}{\partial z} + \frac{i}{2k_p} \Delta_{\perp} \epsilon_p = - \left[g \frac{\omega_p}{\omega_s} |\epsilon_s|^2 + \frac{\alpha_p}{2} \right] \epsilon_p; \quad (1)$$

$$\frac{\partial \epsilon_s}{\partial z} + \frac{i}{2k_s} \Delta_{\perp} \epsilon_s = \left[g |\epsilon_p|^2 - \frac{\alpha_s}{2} \right] \epsilon_s, \quad (2)$$

where the z axis is oriented along the direction of propagation of the beam; Δ_{\perp} is the transverse Laplacian; $\omega_{p,s}$ and $k_{p,s}$ are the frequencies and wave numbers of the incident radiation and the Stokes component (in the case of SRS $\omega_p - \omega_s = \omega_k$, where ω_k is the frequency of the vibrational (or rotational) transition of the molecule); $g = \frac{2N\lambda_s^2\lambda_p}{\pi h \Delta\omega_k n_p n_s^2} \cdot \frac{d\sigma}{d\Omega}$ is the gain for the Stokes wave with $|\epsilon_p| = 1$; N is the number density of molecules along the path; $\Delta\omega_k$ is the line width of the vibrational transition; $n_{p,s}$ and $\lambda_{p,s}$ are the Index of refraction and the wavelength at the frequencies $\omega_{p,s}$; $d\sigma/d\Omega$ is the differential cross section for spontaneous Raman scattering, α_p and α_s are the attenuation coefficients for the incident radiation and the Stokes component, respectively; and, h is Planck's constant.

The equations are written in a coordinate system moving together with the pulse. The saturation-induced change observed in the populations of the Raman-active transition at very high radiation intensities ($I > 10^2$ GW/cm²) is not taken into account in these equations. It is assumed that the vibrations of the molecules follow the change in the amplitudes of the fields and that owing to the dispersion of their group velocities the incident radiation pulse and the Stokes component do not separate along the path. These assumptions are valid for pulse widths $t \ll \left(1/\Delta\omega_k, \frac{L}{C} |n_p - n_s| \right)$, where L is the length of the path.

The effect of SRS on the energy characteristics of a square laser pulse of width $t_p = 10^{-6}$ s propagating in the atmosphere was studied based on the numerical method.¹⁰ Stimulated Raman scattering on vibrational transitions of nitrogen molecules ($\nu_k = \omega_k/2\pi c = 2330$ cm⁻¹) was studied.

At the start of the path ($z = 0$) the profile of the collimated incident beam is gaussian (the effective radius of the beam $r_0 = 10$ cm). The initial pulse energy $E_{p0} = \pi r_0^2 t_p J_0$, where J_0 is the initial intensity on the axis of the beam. The seed for the Stokes component in the medium and its Boundary is the spontaneous Raman scattering noise⁵ in the diffraction divergence cone with initial intensity $|\varepsilon_{s0}|^2 = \frac{\pi \hbar \lambda_p^2 \Delta \omega_k}{2 r_0^2 \lambda_s^3}$. The number density of the molecules and the temperature in the medium, which determine the linewidth $\Delta \omega_k$, are functions of H .^{6,7} In the calculations the width of the Voigt line profile was

used for $\Delta \omega_k$. The quantity $d\sigma/d\Omega$ was determined from the formula⁸ $\frac{d\sigma}{d\Omega} = \frac{A v_s^4}{(v_1^2 - v_p^2)^2}$, where $A = 3.02 \cdot 10^{-28}$ cm²/sr, $v_1 = 8.95 \cdot 10^{-4}$ cm⁻¹, and $v_{p,s} = \omega_{p,c}/2\pi c$. The attenuation coefficients for the components of the radiation in the atmosphere were determined in Ref. 9. Table I gives the parameters for solving numerically the system of equations (1)–(2), describing the propagation of a laser pulse along horizontal paths of length 140 km at an altitude H above the earth's surface.

TABLE 1. The parameters for the numerical solution of Eqs. (1) and (2)

λ_p , μm	H , km	$g \cdot 10^{-9}$, cm ² /erg	$ \varepsilon_{s0} ^2 \cdot 10^{-15}$, erg/cm ³	$\alpha_p \cdot 10^{-8}$, cm ⁻¹	$\alpha_s \cdot 10^{-8}$, cm ⁻¹
1.06	5	1.185	0.828	4.7	4.27
	20	0.966	0.126	0.225	0.246
0.53	5	3.436	2.61	16	10.9
	20	2.802	0.397	1.78	1.137

The computational results for the case of the propagation of neodymium laser radiation ($\lambda_p = 1.06$ μm) on a path at an altitude of 5 km are presented in Fig. 1, where the redistribution of the pulse energy

approximately equal to the energy expended on the excitation of molecules in the process of SRS.

$$E_{p,s} = \frac{c}{2} \int_0^\infty \int_0^\infty |\varepsilon_{p,s}(z, r, t)|^2 r dr dt, \tag{3}$$

where r is the transverse coordinate, between the components of the radiation is shown. One can see that if at the start of the path the energy of the incident radiation $E_{p0} \leq 250$ J, SRS does not occur and the change in the energy of the incident radiation on the path is determined virtually completely by the losses. As E_{p0} increases SRS appears and strongly affects the redistribution of energy between the components of the radiation. For $E_{p0} \geq 500$ J the energy of the incident radiation is practically completely exhausted already on the first half of the path; aside from the losses in the medium part of the energy, proportional to ω_k/ω_p , is extended on the excitation of molecules in the process of SRS, and the rest of the energy, proportional to ω_s/ω_p is converted into the Stokes component, which then propagates with its own attenuation coefficient. The difference between the energies of the incident pulse (curve 1) and the Stokes pulse (curves 4 and 5) on this section of the path is

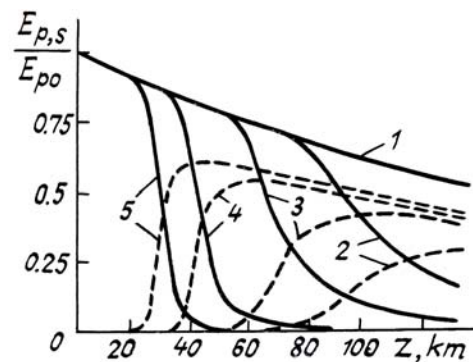


FIG. 1. The redistribution of the energy $E_{p,s}$ between the radiation components on the propagation path for $r_0 = 10$ cm, $t_p = 10^{-6}$ s, and different initial pulse energies $E_{p0} = 250$ (1), 330 (2), 377 (3), 500 (4), and 660(5) J. The solid lines are for the incident radiation E_p with $\lambda_p = 1.06$ μm ; the dashed lines are for the Stokes radiation E_s , $\lambda_s = 1.408$ μm .

The effect of SRS is strongest on sections of the path where the energy in the Stokes component is equal to the energy of the incident radiation. On these sections SRS is the dominant process determining the change in the energy of the incident radiation. Here the nonlinear character of this process is clearly

manifested. It should be kept in mind that the dependences presented in Fig. 1 represent averages over time and over the cross section of the beam. The efficiency of SRS depends on the intensities of the incident radiation and the Stokes component, the change in which is affected by, aside from the SRS, both the attenuation of radiation on the path and diffraction spreading of the beam.

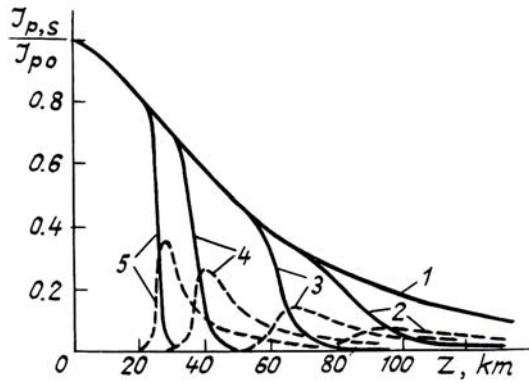


FIG. 2. The intensity of the incident radiation I_p and the Stokes component I_s on the axis of the beam along a path for $r_0 = 10$ cm, $t_p = 10^{-6}$ s, and different initial intensities of the incident radiation $I_{p,0} = 0.8$ (1), 1.05 (2), 1.2 (3), 1.6 (4), and 2.1 (5) MW/cm². The solid lines are for the incident radiation I_p with $\lambda_p = 1.06$ μ m; the dashed lines are for the Stokes radiation I_s with $\lambda_s = 1.408$ μ m.

Figure 2 shows the change in the intensity of the incident radiation and the Stokes component

$$I_{p,s} = \frac{c}{4\pi} |\epsilon_{p,s}|^2$$

on the axis of the beam along the path.

One can see that the decrease in I_p on the starting section of the path is caused by the attenuation of radiation in the atmosphere; this is followed by a rapid decrease in the intensity caused by diffraction of the beam. The Stokes beam formed on the starting section of the path and in the zone of efficient SRS, where the Stokes component rapidly grows up to the maximum, is also affected by the decrease in the intensity I_s owing to losses in the atmosphere and diffraction. The higher the initial intensity I_{p0} is the more rapidly the intensity I_s of the Stokes beam formed decreases. Therefore, a "sharper" Stokes beam forms in a stronger pulse of incident radiation; in other words, the effective radius of the Stokes beam decreases as I_{p0} increases.

On the starting section of the path, where the diffraction of the beam and the effect of the Stokes component on the incident radiation can be neglected, the following expression can be derived for $I_s(r, z)$ from Eqs. (1) and (2):

$$I_s(r, z) = I_{s0} \exp \left[2g |\epsilon_{p0}|^2 e^{-\alpha_p z} - \frac{1 - e^{-\alpha_p z}}{\alpha_p} - \alpha_s z \right], \tag{4}$$

where $r = r/r_0$ and I_{s0} is the intensity of the noise at the Stokes frequency ω_s . From this formula it follows that the intensity of the Stokes component will increase if the threshold condition $I_p > I_{th} = c\alpha_s/8\pi g$ is satisfied. This threshold condition for SRS also follows from Eq. (2). In the case of a gaussian incident beam SRS develops only in the beam channel bounded

by the radius $r < \sqrt{-\ln \left(\frac{c\alpha_s}{8\pi g I_{p0}} \right)}$. If for the Stokes

beam the effective radius \bar{r} is defined in the same manner as for a gaussian beam at the e^{-1} level, then from Eq. (4) we obtain

$$\bar{r}_s = \sqrt{-\ln \left[1 - \frac{\alpha_p}{2g |\epsilon_{p0}|^2 (1 - e^{-\alpha_p z})} \right]}. \tag{5}$$

At the start of the path $\alpha_p z \ll 1$, so that

$$\bar{r}_s \approx \sqrt{-\ln \left(1 - \frac{1}{2g |\epsilon_{p0}|^2 z} \right)}, \text{ here } 2g |\epsilon_{p0}|^2 z > 1.$$

From this formula it follows that on the starting section of the path the Stokes beam peaks all the more rapidly the larger the value of $|\epsilon_{p0}|^2$, i.e., the higher the intensity I_{p0} . We note that the Stokes beam (4) formed is not gaussian. Evidently the beam profile will change along the path as a result of diffraction of this beam and the incident beam and primarily owing to a decrease of the gain in the central part, where the incident radiation is primarily depleted. These results are confirmed by the calculations.

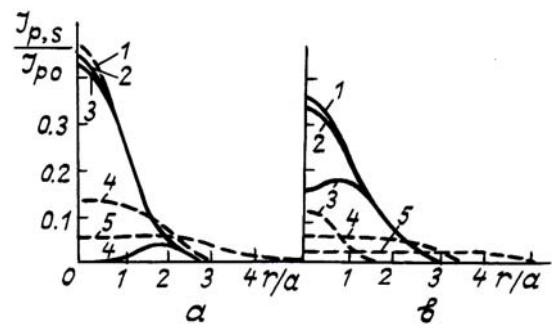


FIG. 3. The distribution in the intensity of the radiation components $I_{p,s}$ in the cross section of the beam located at distances of 51 km (a) and 64.5 km (b) for different starting intensities of the incident radiation on the beam axis $I_{p0} = 0.8$ (1), 1.05 (2), 1.2 (3), 1.6 (4), and 2.1 (5) MW/cm². The solid lines are for the incident radiation I_p with $\lambda_p = 1.06$ μ m; the dashed lines are for the Stokes radiation I_s with $\lambda = 1.408$ μ m.

Figure 3 shows for the cases studied above the distribution $I_{p,s}$ in the cross sections of the beam located at different distances. At a distance of 51 km

for starting pulse energies $E_{p0} = 250, 330,$ and 377 J (curves 1, 2, and 3) the effect of SRS is weak; it increases in the central part of the beam as E_{p0} increases. For $E_{p0} = 500$ J (curves 4) the Stokes beam formed on the starting section of the path has already spread and is significantly different from a gaussian beam – this is the result of intensification of the Stokes component in the channel of the incident beam, which has an annular profile here. In the case $E_{p0} = 660$ J the incident radiation has been virtually completely exhausted, and the Stokes beam (curves 5) has a planar intensity distribution in the central part, right up to $\bar{r} = 2$, and it is significantly wider than the incident beam for the cases 1, 2, and 3.

In Fig. 3b the incident radiation is completely exhausted for the case $E_{p0} = 500$ J also (curve 4), and the profiles of the Stokes beams (curves 4 and 5) have a wide flat top. For $E_{p0} = 377$ J an appreciable Stokes beam has formed, and a dip has appeared at the center of the profile of the incident beam. In the cases $E_{p0} = 250$ and 330 J the decrease in the intensity I_p owing to attenuation of radiation in the atmosphere and diffraction broadening is appreciable (compare with Fig. 3a).

Analysis of the results presented in Fig. 3 shows that the profile of the Stokes beam is formed primarily owing to the nonuniform distribution of the gain of the Stokes component over the cross section of the beam; this gain changes along the path and is related with the change in the profile of the incident beam.

Another factor affecting the Stokes component is the diffraction spreading of the beam. At the start of the path for the incident beam the diffraction length $L_g = 57.6$ km, while the value of L_g for the Stokes beam formed can be several times shorter. Thus for $E_{p0} = 660$ J the diffraction length of the Stokes beam at the distance $z = 23$ km ($L_g = 11.5$ km), where the intensity I_s near the axis is equal to 1% of the intensity I_{p0} , is five times shorter than for the incident beam. For this reason at a distance $z = 51$ km the Stokes beam spreads out substantially (curve 5, Fig. 3a).

The attenuation of the radiation components along the path also effects the Stokes beam. Thus the attenuation coefficient α_s of the Stokes component determines the radius of the channel in which the Stokes component is intensified, while the attenuation coefficient α_p of the incident radiation from Eq. (5) determines the radius of the Stokes beam.

The intensification of the Stokes component is determined the parameter g , whose value depends on λ_p . Simplifying the wavelength dependence of the cross section making the assumption that $\frac{d\sigma}{d\Omega} \sim \frac{1}{\lambda_s}$ and replacing $1/\lambda_s = 1/\lambda_p - 1/\lambda_k$ by $\lambda_k = 1/v_k$, we obtain $g \sim \frac{(\lambda_k - \lambda_p)^2}{\lambda_k^2 \lambda_p}$. Decreasing the wavelength λ_p decreases g and gives rise to SRS at lower intensities I_{p0} and closer to the starting section. Thus using the second harmonic radiation $\lambda_p = 0.53 \mu\text{m}$ of a

neodymium laser gives a 2.9 – fold increase in g (see Table I). A calculation for the starting parameters of the incident radiation used above ($t_p = 10^{-6}$ s and $r_0 = 10$ cm) with $\lambda_p = 0.53 \mu\text{m}$ showed that the region of effective SRS with $E_{p0} = 250$ J was located at a distance z ranging from 20 to 40 km, while for $\lambda_p = 1.06 \mu\text{m}$ in this case SRS did not appear on the path (compare curves 1 in Fig. 1 and Fig. 4).

The results of the calculation of the change in the pulse energy of the radiation components $E_{p,s}$ on paths at different altitudes with the same incident beam at the start of the path ($t_p = 10^{-6}$ s and $r_0 = 10$ cm) are presented for comparison in Fig. 4. As the altitude increases N and $\Delta\omega_k$ decrease. However at altitudes ~ 15 km the ratio $N/\Delta\omega_k$ and therefore also the quantity $g/N\Delta\omega_k$ do not change much. At an altitude of 20 km the parameter g is 1.23 times smaller than at an altitude of 5 km. This causes the region of effective manifestation of SRS to shift (along the path) toward larger values of z compared with the case $H = 5$ km. On high-altitude paths the energy losses in the atmosphere likewise decrease significantly owing to the decrease in $\alpha_{p,s}(H)$.

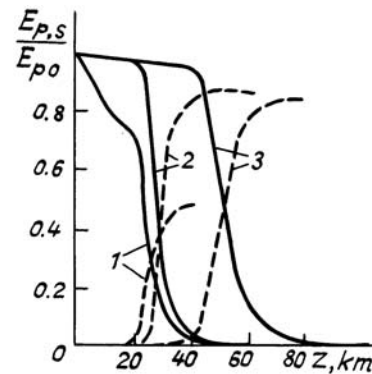


FIG. 4. The change in the energy of the radiation components E_{ps} on paths lying at different altitudes: 1) $H = 5$ km, $E_{p0} = 250$ J; 2) $H = 20$ km, $E_{p0} = 250$ J; 3) $H = 20$ km, $E_{p0} = 150$ J. The solid lines are for the incident radiation I_p with $\lambda_p = 0.53 \mu\text{m}$; the dashed lines are for the Stokes radiation E_s with $\lambda_s = 0.605 \mu\text{m}$.

Thus SRS significantly affects the redistribution of the energy in high-power laser pulses between the Stokes component and the incident radiation. For radiation intensities of the neodymium laser ($\lambda_p = 1.06 \mu\text{m}$) $I_{p0} > 0.8 \text{ MW/cm}^2$ SRS is the dominant process on definite sections of the path and determines the rapid decrease in the intensity of the incident beam and the increase in the intensity of the Stokes component. The Stokes beam forms on the starting sections of the path and in the region of efficient SRS. After the energy of the incident beam is exhausted the Stokes beam diverges in space significantly more rapidly than the incident beam is diffracted. SRS becomes stronger as the wavelength of the incident radiation decreases. Stimulated Raman scattering is also appreciable on long

high-altitude paths. In many problems in atmospheric optics SRS can be regarded as mechanism for nonlinear losses that determines the significant change in the shape of high-power laser pulses and the distribution in the intensity in the transverse cross section of the beam on long paths.

REFERENCES

1. V.P. Sadovnikov, G.M. Strelkov, and M.F. Shalyaev, in: *Abstracts of Reports at the Fourth All-Union Meeting on a Laser Radiation Spreading in a Disperse Medium*, Obninsk-Barnaul, IAM, **2**, 173 (1988).
2. A.D. Hinkley, [ed.], *Laser Monitoring of Atmosphere* [in Russian, Mir, Moscow, (1979)].
3. V.S. Averbakh, A.A. Betin, V.A. Gaponov et al., *Izv. Vyssh. Uchebn. Zaved. SSSR, Ser. Radiofizika*, **21**, No. 8, 1077 (1978).
4. A.A. Betin, G.A. Pasmanik, and L.V. Piskunova, *Kvant. Elektron.*, **2**, No. 11, 2403 (1975).
5. N. Bloembergen, *Nonlinear Optics* New-York, (1965) [Russian translation, Mir, Moscow (1966)].
6. V.E. Zuev and V.S. Komarov, *Statistical Models of the Temperature and Gaseous Components of the Atmosphere* (Gidrometeoizdat, Leningrad, 1986).
7. I.I. Ippolitov, V.S. Komarov, and A.A. Mitsel, *Spectroscopic Methods of Atmospheric Sounding* (Nauka, Novosibirsk, 1985).
8. W.K. Bischel and G. Black, *AIP Conference Proceedings "Eximer Laser — 1983"*, New-York, No. 3, (1983), pp. 181–186.
9. M.S. Kiseleva, I.N. Reshetnikova, and E.D. Fedorova, *Izv. Akad. Nauk SSSR, FAO*, **17**, No. 4, 429 (1981).
10. M.P. Gordin, V.P. Sadovnikov, and G.M. Strelkov, *Radiotekh. Elektron.*, **30**, 1249 (1985).